Towards a better understanding of electrical relaxation

Sabine Kruschwitz[1], Matthias Halisch[2], Carsten Prinz[3], Andreas Weller[4], Mike Müller-Petke[2], Raphael Dlugosch[2]

[1] Bundesanstalt für Materialforschung und –prüfung, Unter den Eichen 87, 12205 Berlin and Technische Universität Berlin, Gustav-Meyer-Allee 25, 13355 Berlin, Germany
[2] Leibniz Institute for Applied Geophysics (LIAG), Stilleweg 2, 30655 Hannover, Germany
[3] Bundesanstalt für Materialforschung und –prüfung, Unter den Eichen 87, 12205 Berlin, Germany
[4] Clausthal University of Technology, Institute of Geophysics, Arnold-Sommerfeld-Straße 1, 38678 Clausthal-Zellerfeld, Germany

This paper was prepared for presentation at the International Symposium of the Society of Core Analysts held in Vienna, Austria, 27 August – 1 September 2017

ABSTRACT

Other than commonly assumed the relaxation times observed in the electrical low-frequency range (1 mHz – 40 kHz) of natural porous media like sandstones and tuff stones cannot be directly related to the dominant (modal) pore throat sizes, measured (e.g.) with mercury intrusion porosimetry (MIP). Working with a great variety of sandstones from very different origins and featuring great variations in textural and chemical compositions as well as in geometrical pore space properties, it was observed that particularly samples with narrow pore throats were characterized by long (low-frequency) relaxations. These, however, can (following the current theories) be rather explained by long "characteristic length scales" in these media or low diffusion coefficients along the electrical double layer. However, there is no straightforward way (or single approved method) of getting reliable numbers for properties such as the lengths of pore throats, the diameter and length of the wide pores and their respective distributions. Consequently we follow a multi-methodical approach and combine the benefits of MIP, micro-computed tomography (µ-CT) and nuclear magnetic resonance (NMR) to achieve much deeper insight due to the different resolutions and sensitivities to either pore constrictions (throats) or wide pores. This helps us to understand, whether the observed electrical relaxation phenomena actually depend on geometric length scales or rather on other properties such as chemical composition, clay content, clay type or cation exchange capacity. In this paper, we showcase selected results of a systematic study of a total of 16 sandstones and three tuffs. Findings and the particular advantage of the used method combination are discussed and shown in detail for a representative sample selection.

INTRODUCTION

Many recent approaches in geophysics and hydrogeophysics try to use the characteristic relaxation time of electrical low-frequency or so called spectral induced polarization (SIP) measurements to derive information on properties such as hydraulic properties (Börner et

al. 1996, Hördt et al. 2009, Weller et al. 2016), effective permeability (e.g. Binley et al. 2005; Weller et al. 2015) or pore size distribution (Revil and Florsch 2010; Florsch et al. 2014). Based on the theory of Schwartz (1962), who related the low-frequency dispersion of colloidal particles in electrolytes to the particle sizes of the grains, it has been intensively discussed amongst geophysicists, how to interpret and relate relaxation phenomena in electrolyte saturated solid matter, i.e. porous natural rocks such as sandstones, tuffs, limestones etc. Some researchers reported on power-law relationships between the electrical relaxation time and the modal pore throat size measured with MIP for their samples (e.g. Scott and Barker 2003; Kruschwitz et al. 2010, Titov et al. 2010). Others argued that rather the length of narrow pore constrictions determine the polarization and hence, relaxation properties. This so called membrane polarization theory has also been implemented in recent numerical modelling approaches (Bücker and Hördt 2013a and 2013b). Kruschwitz et al. 2016 studied this highly debated relationship between the electrical relaxation time τ and the modal pore throat size compiling the largest and most diverse data set as yet. Including published and unpublished sources they worked with geological materials from very different areas with a wide variation of dominant pore throat sizes, specific surface areas, porosities and permeabilities. Their aim was to systematically study the question of what is the characteristic textural length scale controlling low-frequency relaxation and hence the frequency of the peak phase.

In conclusion Kruschwitz et al. 2016 could divide the large group of samples into three groups as illustrated in Fig. 1. The graph shows the measured SIP relaxation times τ_{peak} as a function of dominant (model) pore throat size D_{dom} determined with MIP. In this graph we can distinguish three groups of samples. The first group ("type 1" samples) simply follow the "predicted" behavior and feature relaxation times that might be controlled by the modal pore throat sizes of the samples. A representatives of type 1 samples is for example Bentheimer sandstone. The second group ("type 2" samples) consists of rocks, that likewise seem to follow the predicted $\tau_{peak} \sim D_{dom}$ relationship, but at the same time show a low-frequency relaxation (large τ_{peak} values), that cannot be explained by the very small pore throat sizes measured with MIP. A representative of this type 2 samples is Langenauer sandstone. These materials show a so-called "double-peak" SIP behavior, because they show two separate relaxation processes in the SIP data and accordingly are addressed by two τ_{peak} values, whereas their pore spaces are characterized by only one dominant pore throat size in the MIP. For these samples as well as for those belonging to the third group ("type 3" samples), which do not follow the predicted $\tau_{peak} \sim D_{dom}$ relationship at all, but show very slow SIP relaxation processes even though the dominant pore throat sizes are mostly smaller than 5 µm. These findings raised anew and rather desperately the question what is really controlling the low-frequency relaxation time in porous solid media. From a theoretical, electrochemical point of view it should rather be the lengths of pores, not the diameter. The reason why still a dependency on the pore throat diameters was observed (for type 1 and party type 2 samples) could be that for these materials the pore throat lengths are relatively equal in size compared to their diameters.

This requires though, that we characterize the pore systems in much more detail than it has been done with MIP so far. Only a better comprehension of the characteristic length scales present in a pore space will help to understand what is causing the measured SIP relaxation phenomena. For Langenauer sandstone for example we would expect (additionally to the pore throat size) a second characteristic length of about 20 – 150 µm to explain the high relaxation time of ca. 5.3 s (marked in Fig. 1). In this study we follow a multi-methodical approach and apply µ-CT and NMR on the majority of the same samples as shown above. As all these methods are sensitive to other pore space properties and have different resolutions which is beneficial to fully leverage their potential by combining them.

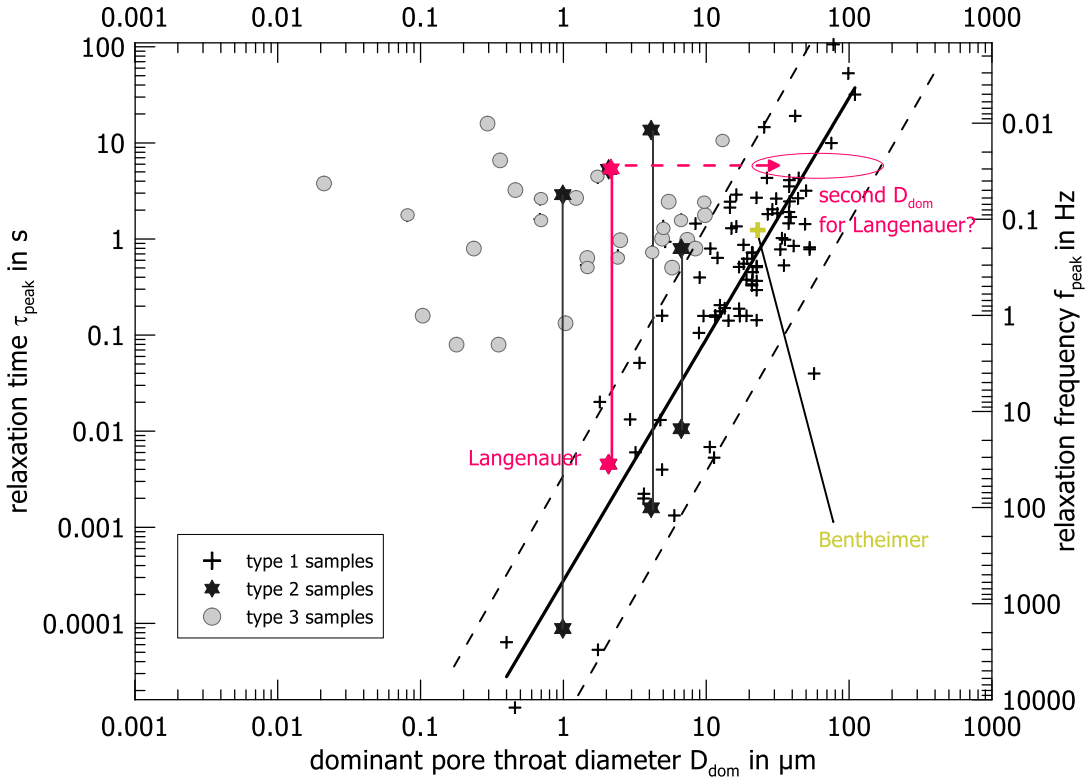

Figure 1: Characteristic relaxation times τ_{peak} from SIP versus dominant modal pore throat size D_{dom} determined with MIP (modified after Kruschwitz et al. 2016).

SAMPLES & METHODOLOGY

For our comparison of the pore space characteristics, two different rocks have been selected for presentation in this paper: Bentheimer sandstone and Langenauer sandstone (marked in Fig. 1). Bentheimer sandstone is a Berea type sandstone that has been used and described in many previous petrophysical studies. The shallow-marine material was deposited during the Early Cretaceous and is quarried near Bad Bentheim and Gildehaus, Germany. It is a fine to medium grained sandstone of white to yellowish or light red color. Bonding is mostly due to grain-grain cohesion (Dubelaar and Nijland, 2014). Langenauer sandstone (sometimes referred to as Dlugopole oder Wünschelburger sandstone) originates from the

Upper Cretaceous, and recent outcrops can be found in the vicinity of Dlugopole, a few kilometers south of Wroclaw, Poland. It is a medium grained, white-yellowish sandstone. Scanning electron microscopy images for both materials are shown in figure 2, also indicating the presence of caolinite as dominant clay mineral (10.5 vol.-% for the Bentheimer, and 8.5 vol.-% for the Langenauer sandstone, according to quantitative X-ray diffraction analysis).

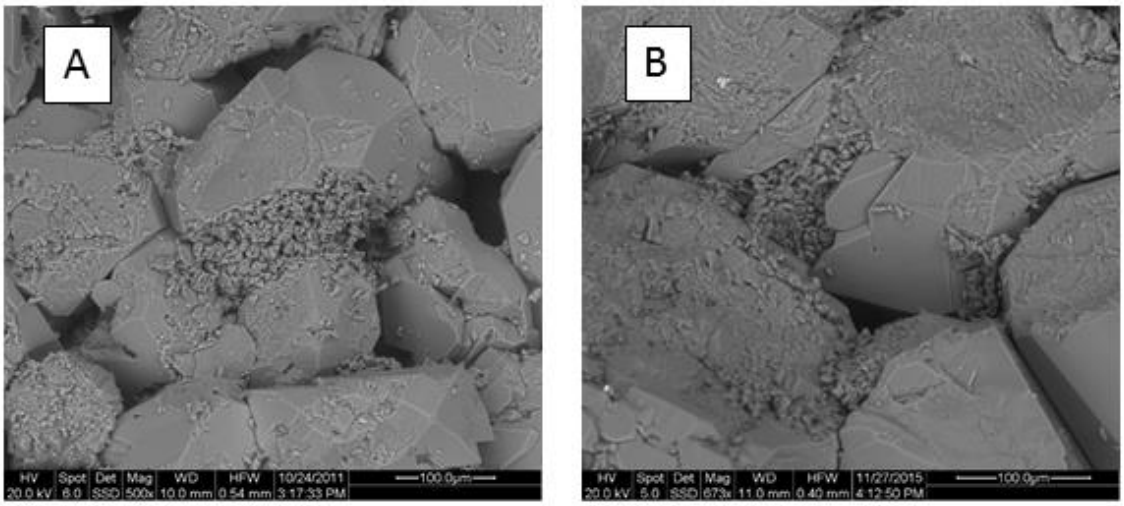

Figure 2: SEM images of Bentheimer sandstone (A) and Langenauer sandstone (B).

Mercury intrusion porosimetry measurements were conducted using an AutoPore III from Micromeritics. The pressure range of the AutoPore system from 0.004 - 400 MPa corresponds to pore sizes of ca. 400 µm down to 3.6 nm. The cumulative intruded mercury volume versus pressure curves were converted to a differential intrusion (in ml/g) versus pore diameter (in µm) assuming cylindrical pores using the Washburn equation. The dominant pore throat sizes are the modal pore throat sizes and were calculated from the maximum value in the differential intrusion over pressure curves. The µ-CT imaging has been performed with a nanotom 180 S (GE Sensing & Inspection Technologies), a high-resolution X-ray CT system. The minimum focal spot size is 0.6 µm, which is optimal for pore structure analyses of small cylindrical samples with diameters of 1 mm at a length of 5-10 mm. Voxel resolutions of 1.25 – 2.0 µm could be achieved. The digital image analysis (DIA) workflow has been extensively described by Schmitt et al. (2016) and Halisch et al. (2016). The NMR measurements were carried out with a Magritek Core Analyzer (Magritek, Wellington, New Zealand) operating at a Lamor frequency of 2 MHz. We use a CPMG pulse sequence with an echo spacing of 200 µs and the built-in cooling/heating system ensures a constant sample temperature between 21°C and 22°C during the measurements. The porosity of the fully saturated samples (for NMR and SIP the very same samples could be used) has been determined by calibration with a bulk water sample of known dimension. The smooth relaxation time distributions are derived using a common multi-exponential approach. A regularization parameter is used to weigh the minimum structure in the relaxation time distribution and the minimum

residual between the measured data and model response (e.g., Whittall et al., 1991). A pore size distribution is finally calculated assuming fast-diffusion and cylindrical pores as (Brownstein and Tarr, 1979):

$$d = 4\rho T_2 \quad (1)$$

with d being the pore size, ρ the surface relaxivity, and T_2 the transverse relaxation time.
The SIP measurements were carried out in the laboratory using a SIP-ZEL device (Zimmermann, 2008). The system allows for two simultaneous 4-point measurements over a frequency range from 1 mHz to 45 kHz. The measurements were carried out at 27 logarithmically equidistant steps in the frequency range. The sample holder used has been manufactured at BAM and has been described elsewhere, for example in Kruschwitz (2008). A spectrum of measured electrical impedances is obtained and usually recorded either as magnitude $|\rho|$ and phase ϕ, or as real (ρ') and imaginary (ρ'') part of the resistivity respectively. All samples in this study show a peak relaxation behavior, which means that the phase or more precisely the imaginary part of the resistivity exhibits a clear maximum at a certain frequency. Like in other studies we work with the peak relaxation time τ_{peak}, which is $1/(2\pi f_{peak})$, with f_{peak} being the frequency, where the quadrature resistivity is maximal.

RESULTS

For the purpose of clarity we chose a common representation of the results of all methods in one diagram. We plot pore volume distributions and systematically regard the fractions of porosity (here added together from large to small pore sizes) that are covered in each part of the curves. In case of µ-CT we use the volumes of the equivalent diameter distributions. In the following we summarize our observations for two investigated sandstones.

Bentheimer sandstone (sample Bh5, Fig. 3):

The MIP displays a narrow unimodal distribution of pore throats with a dominant size around 39 µm. For the µ-CT the maximum resolution was a voxel size of 1.75 µm. The biggest part of the total porosity contained in pore with an equivalent diameter of ca. 125 µm. Using a surface relaxivity of 37.5 µm/s the NMR T2 spectrum covers reasonably well the equivalent diameter volume curves as calculated in the DIA, its maximum appears then at ca. 85 µm. Adding together the porosities that the methods capture from the wide pores to the small pores (thresholds Φ given in Fig. 3 on top), we find that MIP clearly cannot see the wider pore fractions that are recorded in the DIA. In a regular pore throat-pore body system this is to be expected as the MIP always addresses the pore body volumes to the respective throats sizes that provide entry to them. This is why the porosities with MIP and µ-CT are significantly different for pores ≥ 45 µm, but tend to be more in the same range for pores ≥ 10 µm. The NMR seems to be influenced by both the wider pores and the smaller throats. The total porosities determined by NMR and MIP are with ca. 23% in good agreement, gravimetrically we determined 23.3%. When we use the equivalent diameter and NMR distributions to calculate from their arithmetic mean a proxy characteristic length scale for the wide pores we get about 105 µm. This results in a pore throat to pore body ratio of ca. 1:2.7. It should be noticed that the position of the NMR

spectrum and hence the surface relaxivity ρ has been chosen so that it fits and mostly covers the frequency distribution of the equivalent pore diameters determined by µ-CT. It is conceivable that NMR is more strongly influenced by the larger pores and should be shifted further right in this diagram covering more the width, breadth or even length distributions (compare Zhang et al. 2017). Similar analysis of further samples will help to improve our knowledge of how to correlate these distributions.

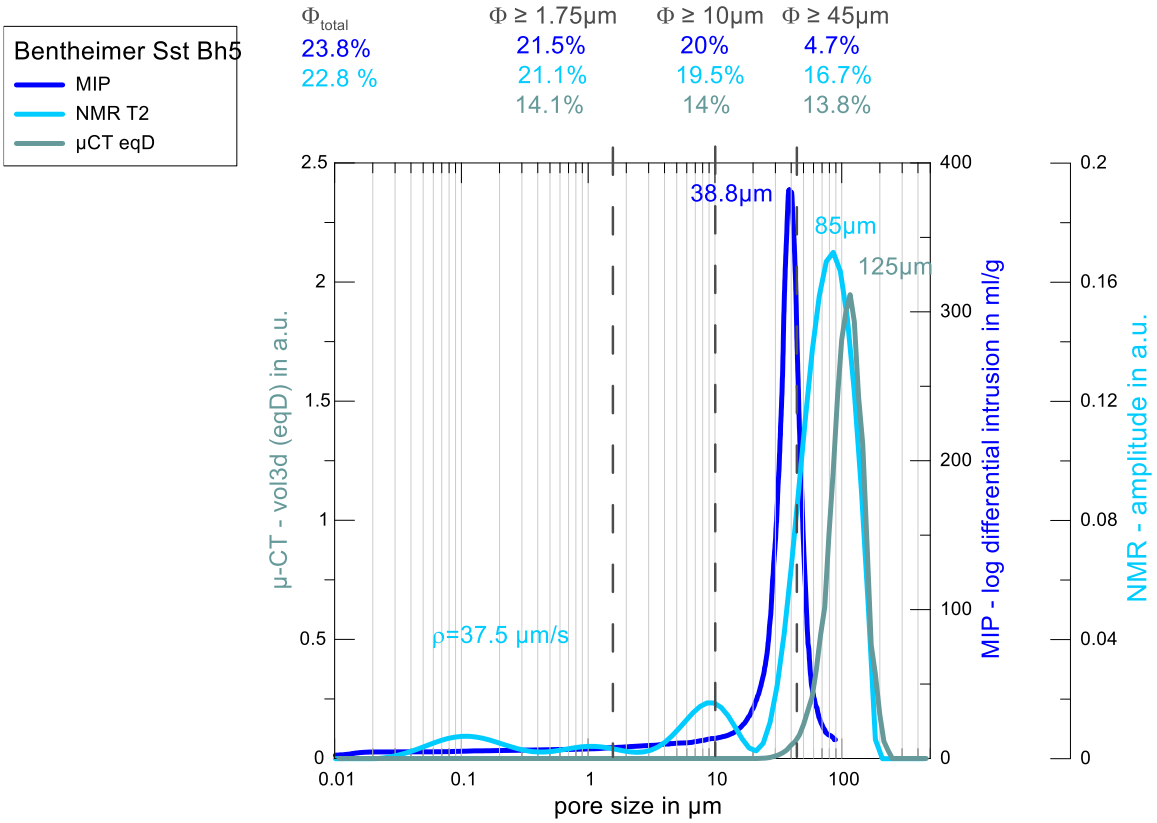

Figure 3: Bentheimer sandstone, pore size distributions as determined with MIP (dark blue), NMR (light blue) and µ-CT equivalent diameter (green) and cumulative porosities for three different pore fractions.

Langenauer sandstone (Fig. 4):

Similar to Bentheimer sandstone also Langenauer sandstone has a uni-modal MIP pore size distribution, here with a peak at ca. 2 µm. The µ-CT curve however identifies big pores in the range around 75 µm. The porosity identified for pores ≥ 8 µm is 6.9%, which is much higher than what is seen with MIP for this pore size. The NMR T2 spectrum indicates a bi-modal distribution supporting both the µ-CT and MIP data well when a surface relaxivity of 30 µm/s is assumed. Looking at the porosities, NMR identifies with 5.8% slightly more volume in the wide pore region (pore size ≥ 8µm) as compared to the pore throat region (pore sizes between 1.25 and 8 µm), where additional porosity of 3.8% are detected. More clearly than for the Bentheimer sandstone the NMR signal seems to be influenced by both the wide and the small throats. The total porosities of 12% (MIP) and 12.1% (NMR) correspond well to the 11.7% measured gravimetrically. Calculating with a mean value of 60 µm (mean of NMR and µ-CT peaks) for the wide pores, the pore throat to body ratio

for Langenauer sandstone is about 1:30. Compared to the Bentheimer sandstone Langenauer sandstone has a more heterogeneous pore system that is clearly dominated by two very different length scales. A wide pore size of around 60 µm convincingly explains the low frequency relaxation in SIP (compare Fig. 1).

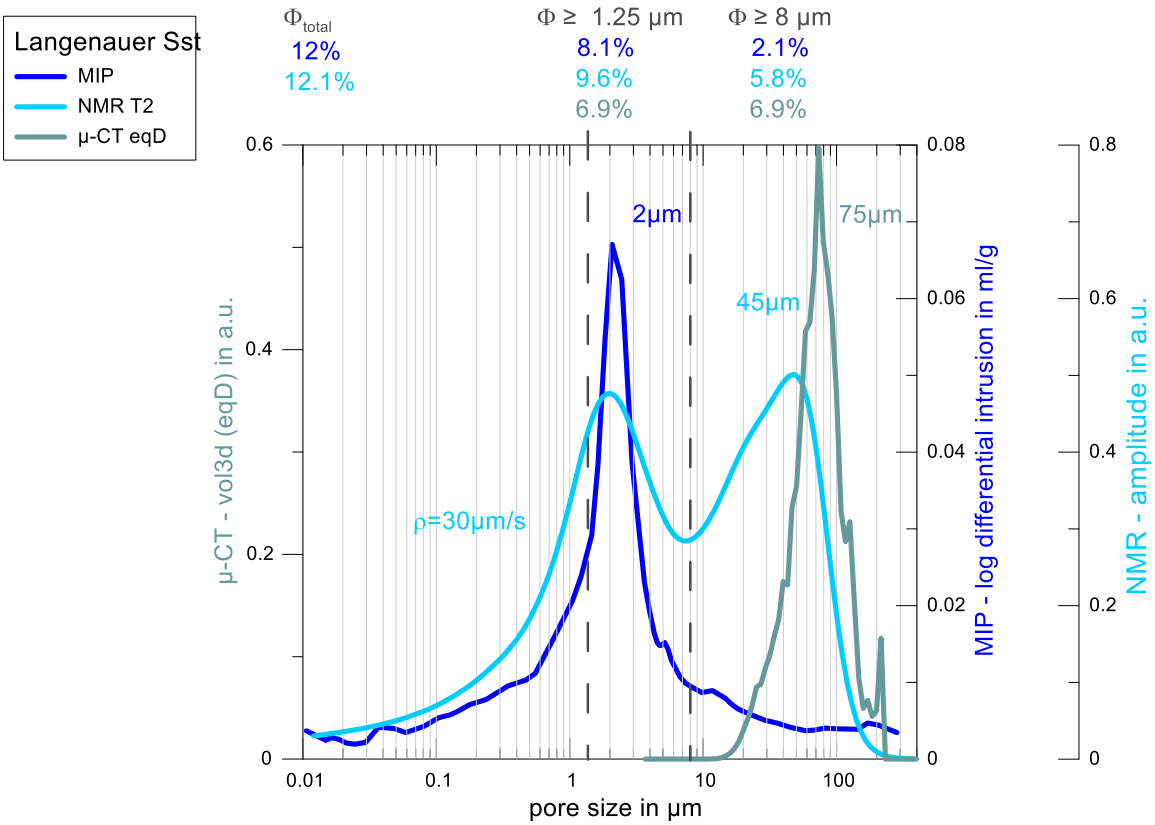

Figure 4: Langenauer sandstone, pore size distributions as determined with MIP (dark blue), NMR (light blue) and µ-CT equivalent diameter (green) together with cumulative porosities for three different pore fractions.

CONCLUSION

In this paper we present an important contribution towards a better understanding of SIP relaxation phenomena due to an enhanced characterization of complex pore systems in solid media using MIP, µ-CT and NMR. Samples with fairly uniform pore geometries are observed to follow the predicted power law relationship of SIP relaxation time τ_{peak} and dominant pore throat size D_{dom} as determined with MIP. In these uniform pore spaces the size ratios of pore throats to pore bodies are moderate, here ca. 1:3 for Bentheimer sandstone. Samples where two SIP relaxation processes are observed seem to be characterized by more extreme ratios of throat to body sizes. For the investigated Langenauer sandstone we get a ratio ca. 1:30. Presumably one relaxation can be attributed to the so-called active zone in the pore throat and another one to the length of the pore body.

REFERENCES

1. Börner, F., J. Schopper, and A. Weller, "Evaluation of transport and storage properties in the soil and groundwater zone from induced polarization measurements", *Geophysical Prospecting (1996)*, **44(4)**, 583-601.
2. Hördt, A., R. Blaschek, F. Binot, A. Druiventak, A. Kemna, P. Kreye, and N. Zisser, "Case histories of hydraulic conductivity estimation with induced polarization at the field scale", *Near Surface Geophysics (2009)*, **7 (5-6)**, 529-545.
3. Weller, A., Z. Zhang, L. Slater, S. Kruschwitz, and M. Halisch, "Induced polarization and pore radius — A discussion", *Geophysics (2016)*, **81(5)**, D519-D526.
4. Binley, A., L. Slater, M. Fukes, and G. Cassiani, "Relationship between spectral induced polarization and hydraulic properties of saturated and unsaturated sandstone", *Water Resources Research (2005)*, **41**, W12417.
5. Weller, A., L. Slater, A. Binley, S. Nordsiek, and A. Xu, "Permeability prediction based on induced polarization: Insights from measurements on sandstone and unconsolidated samples spanning a wide permeability range", *Geophysics (2015)*, **80 (2)**, D161-D173.
6. Revil, A. and N. Florsch, "Determination of permeability from spectral induced polarization in granular media", *Geophysical Journal International (2010)*, **181**, 1480–1498.
7. Florsch, N., A. Revil, and C. Camerlynck, "Inversion of generalized relaxation time distributions with optimized damping parameter", *Journal of Applied Geophysics (2014)*, **109**, 119-132.
8. Scott, J., and R.D. Barker, "Determining pore throat size in Permo- Triassic sandstones from low-frequency electrical spectroscopy*". Geophysical Research Letters (2003)*, **30**, 1450–1453.
9. Kruschwitz, S., A. Binley, D. Lesmes, and A. Elshenawy, "Textural controls on low frequency electrical spectra of porous media", *Geophysics (2010)*, **75 (4)**, WA113–WA123.
10. Titov, K., A. Tarasov, Y. Ilyin, N. Seleznev, and A. Boyd, "Relationships between induced polarization relaxation time and hydraulic properties of sandstone", *Geophysical Journal International (2010)*, **180**, 1095–1106.
11. Bücker, M., and A. Hördt, "Long and narrow pore models for membrane polarization", *Geophysics (2013a)*, **78 (6)**, E299 – E314.
12. Bücker M., and A. Hördt, "Analytical modelling of membrane polarization with explicit parametrization of pore radii and the electrical double layer", *Geophysical Journal International (2013b)*, **94**, 804-813.
13. Kruschwitz, S., C. Prinz, and A. Zimathies, "A Study into the correlation of dominant pore throat size and SIP relaxation frequency", *Journal of Applied Geophysics (2016)*, **135**, 375-386.
14. Dubelaar, W.C., and T.G. Nijland, "The Bentheim Sandstone: geology, petrophysics, varieties and its use as dimension stone", in: Lollino, G., Giordan, D., Marunteanu, C., Christaras, B., Yoshinori, I., Margottini, C. (Eds.), *Engineering Geology for Society and Territory (2014)*, **vol. 8**, Springer International Publishing, Switzerland, 557-563.

15. Schmitt, M., M. Halisch, C. Müller, and C.P. Fernandes, "Classification and quantification of pore shapes in sandstone reservoir rocks with 3D X-ray micro-computed tomography", *Solid Earth (2016)*, **7**, 285-300.
16. Halisch, M., M. Schmitt, and C.P. Fernandes, "Pore Shapes and Pore Geometry of Reservoirs Rocks from µ-CT Imaging and Digital Image Analysis", Proceedings of the Annual Symposium of the Society of Core Analysts (2016), Snowmass, Colorado, USA, SCA2016-093.
17. Whittall, K. P., M.J. Bronskill, and R.M. Henkelman, "Investigation of analysis techniques for complicated NMR relaxation data", *Journal of Magnetic Resonance (1991)*, **95**, 221–234.
18. Brownstein, K. R., and C.E. Tarr, "Importance of classical diffusion in NMR studies of water in biological cells", *Physical Review A (1979)*, American Physical Society, **19 (6)**, 2446-2453.
19. Zimmermann, E., A. Kemna, J. Berwix, W. Glaas, H. Münch, and J. Huisman, "A high accuracy impedance spectrometer for measuring sediments with low polarizability", *Meas. Sci. Technol. (2008)*, **19 (10)**, 105603.
20. Kruschwitz, S., "Assessment of the Complex Resistivity Behavior of Salt Affected Building Materials", Dissertation. Federal Institute for Materials Research and Testing (2008), Berlin, Germany.
21. Zhang, Z., S. Kruschwitz, A. Weller, M. Halisch, and C. Prinz, "Enhanced pore space analysis by use of µ-CT, MIP, NMR, and SIP", Proceedings of the Annual Symposium of the Society of Core Analysts (2017), Vienna, Austria (SCA2017-083).